WESTERN caspian UNIVERSITY

e-ISSN 3105-4293
p-ISSN 3105-4285

Journal of Nanotechnology and Innovative Materials

Vol 1, № 4, 2026

Baku - 2026

Western Caspian University

e-ISSN 3105-4293

p-ISSN 3105-4285

Journal of Nanotechnology and Innovative Materials

Vol 1, No 4, 2026

DOI:10.54414/VWTT8467

https://jnim.wcu.edu.az/

CONTENTS

https://doi.org/10.54414/SFHD5794

Journal of Nanotechnology and Innovative Materials

Research Article

Synthesis and Study of Physical Properties of New Single Crystals of $(Bi_2Te_3)_{1-x}La_x$ Solid Solution

Sayyara A. Nabieva[1], Durdana F. Rustamova[2], Madina F. Nabili[3], and Munawar Abbas[4]

[1]Institute of Physics, Ministry of Science and Education, 131 H. Javid Avenue, AZ1143 Baku, Azerbaijan
[2]Department of Mechanics and Mathematics, School of Advanced Technologies and Innovation Engineering, Western Caspian University, Ahmad Rajabli 17A, III Parallel, AZ1001 Baku, Azerbaijan
[3]First Chayli Secondary School named after Kamil Samadov, Ministry of Science and Education, First Chayli Village, AZ5600 Shamakhi, Azerbaijan
[4]Department of Mathematics, Faculty of Science, Fırat University, 23119 Elazığ, Türkiye

Received: 28.04.2026 Accepted: 08.05.2026 Published: 29.05.2026

https://doi.org/10.54414/GCQH1902

Abstract

In the present study, bismuth telluride (Bi_2Te_3) was selected as the base material due to its well-known thermoelectric characteristics. This semiconductor compound plays a crucial role in applications such as energy conversion, cooling technologies, and waste heat recovery systems. Lanthanum is a rare-earth element. To enhance its functional properties, lanthanum (La) was introduced into the Bi_2Te_3 matrix, forming $(Bi_2Te_3)_{1-x}La_x$ solid solutions. It is an interesting and promising area of research in the field of obtaining single-crystal thermoelectric materials. The investigation of such doped single crystals represents a promising direction for improving thermoelectric efficiency. Lanthanum (La) has been widely employed as a dopant to optimize carrier concentration, modify the crystal lattice, and improve the thermoelectric performance of Bi_2Te_3-based materials. A detailed analysis of the $(Bi_2Te_3)_{1-x}La_x$ system was carried out, including the construction of phase diagrams. It was established that within the composition range x = 0.01–0.05, a solid solution region based on Bi_2Te_3 exists at room temperature. Additionally, a eutectic interaction between Bi_2Te_3 and La was identified at approximately 15 at.% La with a temperature close to 440 °C. Lanthanum doping resulted in measurable changes in the physical properties of Bi_2Te_3 single crystals. The results demonstrate that lanthanum incorporation yields single crystals with enhanced thermoelectric and galvanomagnetic properties, making them attractive for advanced material applications.

Keywords: microsolidity, solid solution, density, single crystal, thermoelectric, photovoltaic, optics, electrical converter

1. Introduction

The rapid progress of modern technologies has significantly increased the demand for novel single-crystal materials. Such materials are widely utilized in semiconductor devices, optoelectronics, photovoltaics, and various branches of applied science.

However, the fabrication of high-quality single crystals remains a complex and resource-intensive process. High synthesis temperatures are generally required for crystal growth. It requires elevated temperatures, strict control of growth conditions, extended processing time, and a high degree of purity. Single crystals are often sensitive to crystal defects and mechanical stresses during fabrication. They are susceptible to structural defects and external mechanical stresses during crystal growth. Monocrystals take a very long time to grow, which increases the production costs of the resulting product. Even minor structural imperfections can adversely affect the performance of the final material.

Bismuth telluride (Bi_2Te_3) is considered one of the most efficient thermoelectric materials currently available. It is formed by combining bismuth and tellurium in a stoichiometric ratio and possesses a rhombohedral crystal structure. Bismuth telluride is commonly used in thermal power converters, cooling systems, and energy recovery. At the same time, it is more widely used in thermoelectric conductors [1], [2], [3]. This structural feature enables its modification through doping with rare-earth elements, which has been reported to improve the thermoelectric performance of Bi_2Te_3-based materials. Previous studies have demonstrated that rare-earth doping can effectively modify the crystal structure and improve the thermoelectric performance of Bi_2Te_3-based materials [4], [5], [6], [7], [8]. The chemical composition of bismuth telluride is as follows: it is a stoichiometric compound consisting of two bismuth atoms and three tellurium atoms. The crystal structure of this material belongs to the rhombohedral class. This structure helps it to obtain promising thermoelectric materials from rare-earth elements, as well as multicomponent phases obtained on their basis. One of the key advantages of Bi_2Te_3 is its ability to exhibit both p-type and n-type conductivity [3]. It combines relatively high electrical conductivity with low thermal conductivity, which is essential for efficient thermoelectric conversion [9]. Taking advantage of these properties, it is used in thermoelectric generators and thermoelectric cooling systems.

In addition, the fact that this crystal has a thermoelectric effect makes its application in the field of electronics indispensable. Due to the Seebeck effect, Bi_2Te_3 can directly convert thermal energy into electrical energy [3]. Its high Seebeck coefficient and figure of merit (ZT) make it a leading material for thermoelectric applications [9]. The Bi_2Te_3 crystal has a high Seebeck coefficient, meaning that a strong electric field is generated when a temperature difference is applied from one side to the other.

2. Materials and Methods

To synthesize alloys of the $(Bi_2Te_3)_{1-x}La_x$ system, the Bi_2Te_3 compound was first synthesized. The alloys in the system were synthesized from elements with the following purities: Bi - 99.999%, Te - 99.999%, La - 99.98%. To conduct a comparative analysis of the obtained single crystal, 1%, 2%, 3%, and 5% La were used. At this time, the mass of the single crystal, Bi_2Te_3 = 417.96 + 382.8 = 800.76 g mol^{-1}, and the mass of the lanthanum, La = 138.91 g, were used.

The mass ratios of the newly purchased monocrystals were as follows:

- 99% Bi_2Te_3 + 1% La = 792.7524 + 1.3891 = 794.1415 g

Bi_2Te_3 = 1.9965 g
La = 0.0035 g

- 97% Bi_2Te_3 + 3% La = 776.7372 + 4.1673 = 780.9045 g

Bi_2Te_3 = 1.9819 g
La = 0.0181 g

- 95% Bi_2Te_3 + 5% La = 760.722 + 6.9455 = 767.6675 g

Bi_2Te_3 = 1.9819 g
La = 0.0181 g

The alloy of the $(Bi_2Te_3)_{1-x}La_x$ system was synthesized from the Bi_2Te_3 compound and the La element in quartz ampoules with air sucked in to a pressure of 0.133 Pa at a temperature range of (700−1000) ^{0}C. The synthesized sample was thermally treated at 500 ^{0}C for 200 hours to bring it to equilibrium. Equilibrium $(Bi_2Te_3)_{1-x}La_x$ solid solution alloys were studied using physicochemical analysis methods.

X-ray diffraction analysis of the obtained alloys was performed on a D2 PHASER X-ray diffractometer. In this case, CuKα radiation and a Ni filter were used as the anode. Microstructural analysis was performed using a MIM-8 microscope. Density was determined by the pycnometric method. Toluene was used as the filling solvent.

3. Results and Discussion

Figure 1 shows the phase diagram of the $(Bi_2Te_3)_{1-x}La_x$ system. The α phase corresponds to a Bi_2Te_3-based solid solution, which remains stable up to approximately 5 at.% La. At higher La concentrations, a two-phase region (α + M) is observed, indicating that the solubility limit of La has been exceeded and a La-rich secondary phase forms. A eutectic reaction occurs at approximately 15 at.% La and 440 °C.

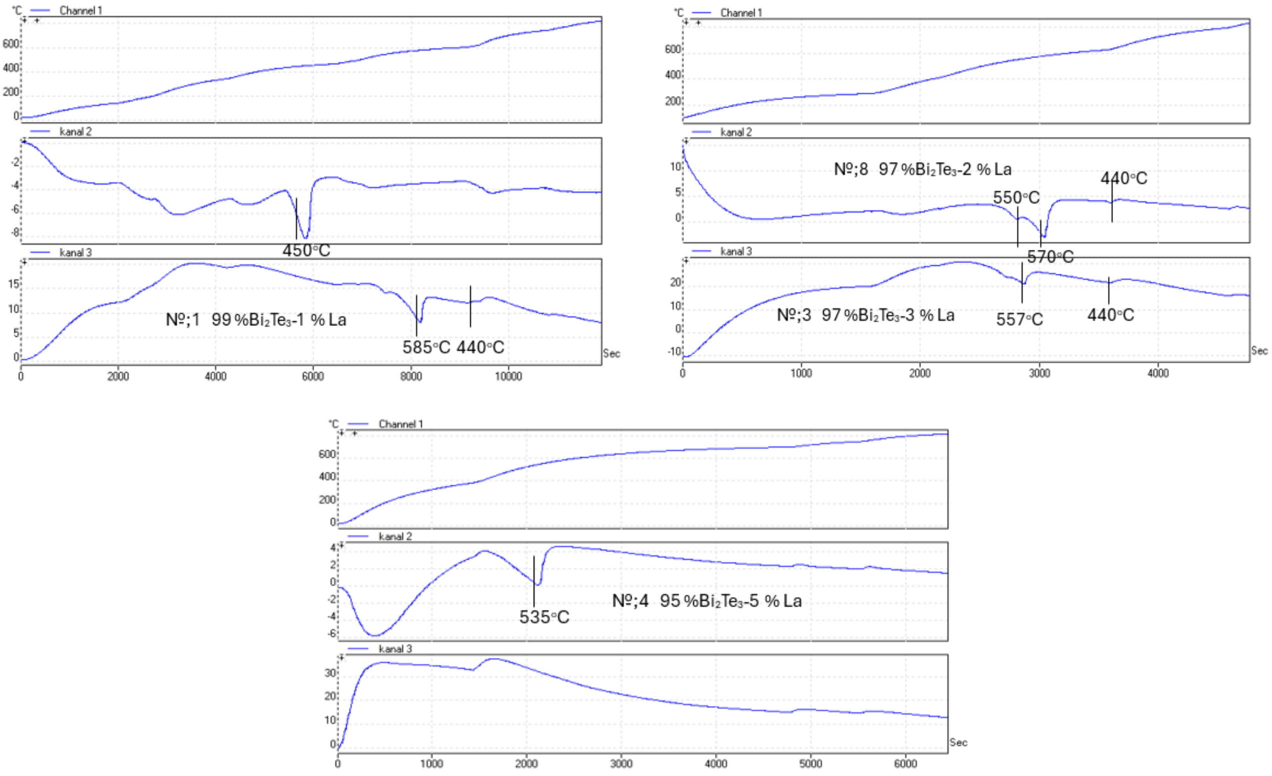

Figure 1. Diagrams of phase equilibria in the $(Bi_2Te_3)_{1-x}La_x$ systems.

The interpretation of the obtained diagrams can be explained as follows. The solvus line (solubility limit) indicates the maximum amount of a rare-earth element that can dissolve in Bi_2Te_3 at room temperature [5], [6], [10].

This interval depends on the radius and electronic structure of the La atom. The eutectic point indicates the lowest melting temperature (between 425–450°C) and the composition corresponding to this temperature (12–15 at.% La). This dependence shows that this temperature and composition depend on the strength of the interaction between the rare-earth element and Bi_2Te_3. The liquidus and solidus curves define the crystallization interval of the system.

The difference between these lines indicates the crystallization interval of the system. As the amount of rare-earth element increases, the melting temperature decreases (to the eutectic point).

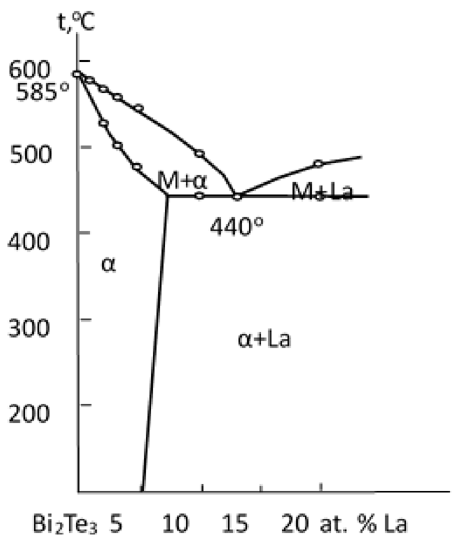

Figure 2. Graphical representation of selected physicochemical properties of the $(Bi_2Te_3)_{1-x}La_x$ (x = 0.01, 0.02, 0.03, and 0.05) alloy system.

X-ray diffraction analysis confirmed the formation of the Bi_2Te_3-based solid solution. The observed shift of diffraction peaks toward lower diffraction angles suggests a slight lattice expansion resulting from the incorporation of La into the Bi_2Te_3 crystal structure. Similar structural changes have been reported for other rare-earth-doped Bi_2Te_3 systems [4], [5], [7], [11], supporting the formation of a substitutional solid solution.

Table 1. Dependence of alloys in the $(Bi_2Te_3)_{1-x}La_x$ systems on composition, DTA, density, and microhardness.

Composition of phases, % $(Bi_2Te_3)_{1-x}(La)_x$ $(Bi_2Te_3)_{1-x}(La)_x$	**Melting temperature, °C**	**Density, g/cm³**	**Microhardness, MPa**
97% Bi_2Te_3-3% La	510.580	8.85	960
95% Bi_2Te_3-5% La	460.575	8.87	970
90% Bi_2Te_3-10% La	440.590	8.88	975
87% Bi_2Te_3-13% La	440	8.90	Eutectic
20% Bi_2Te_3-20% La	440.520	8.91	980

As shown in Table 1, the density increased slightly from 8.85 to 8.91 g cm^{-3} with increasing La concentration, while the microhardness increased from 960 to 980 MPa. These trends suggest that lanthanum incorporation modifies the crystal lattice and improves resistance to localized plastic deformation.

4. Conclusion

In the presented work, a new single crystal was obtained based on the combination of Bi_2Te_3 (bismuth telluride) and La (lanthanum). The modification of its structure through lanthanum doping successfully modified the crystal structure and physical properties.

The conducted study shows that the addition of lanthanum results in limited solubility within the Bi_2Te_3 matrix and leads to the formation of a eutectic-type system. Furthermore, a slight increase in density and microhardness is observed with increasing lanthanum content.

These observations are consistent with structural modifications induced by lanthanum incorporation into the Bi_2Te_3 lattice. The obtained materials demonstrate improved characteristics, indicating their suitability for applications in energy systems, cooling technologies, and advanced electronic devices.

Overall, the Bi_2Te_3–La system represents a promising direction for the development of high-performance thermoelectric materials and functional single crystals.

The Bi_2Te_3 + La compound has great potential in the field of thermoelectric materials development. The research allows optimizing electrical and thermal properties by modifying the nanostructure and crystal structure of the material. This research could lead to more effective applications in the fields of renewable energy, cooling systems, and energy recovery in the future. At the same time, it is possible to produce high-quality sensors, lasers, and other precision research instruments from monocrystals obtained in the fields of chemistry and medicine.

Author Contributions

All authors reviewed, edited, and approved the manuscript.

Conflict of Interest

The authors declare no conflicts of interest.

Funding

This research received no external funding.

Acknowledgment

The authors declare no acknowledgments.

Abbreviations

Bismuth Telluride (Bi_2Te_3), Lanthanum (La), X-ray Diffraction (XRD).

References

[1] Dmitriev AV, Zvyagin IP. Current trends in the physics of thermoelectric materials. Physics-Uspekhi. 2010 Nov 15;53(8):789-803. https://doi.org/10.3367/ufne.0180.201008b.0821

[2] Fang T, Li X, Hu C, Zhang Q, Yang J, Zhang W, Zhao X, Singh DJ, Zhu T. Complex band structures and lattice dynamics of Bi2Te3-based compounds and solid solutions. Advanced Functional Materials. 2019 Jul;29(28):1900677. https://doi.org/10.1002/adfm.201900677

[3] Pei J, Cai B, Zhuang HL, Li JF. Bi2Te3-based applied thermoelectric materials: research advances and new challenges. National science review. 2020 Dec;7(12):1856-8. https://doi.org/10.1093/nsr/nwaa259

[4] Shi X, Ai X, Zhang Q, Lu X, Gu S, Su L, Wang L, Jiang W. Enhanced thermoelectric properties of hydrothermally synthesized n-type Se&Lu-codoped Bi2Te3. Journal of Advanced Ceramics. 2020 Aug;9(4):424-31. https://doi.org/10.1007/s40145-020-0382-9

[5] Yapryntsev MN, Lyubushkin RA, Soklakova ON, Ivanov ON. Synthesis and electrical properties of Bi2Te3-based thermoelectric materials doped with Er, Tm, Yb, and Lu. Semiconductors. 2017 Jun;51(6):710-3. https://doi.org/10.1134/s106378261706029x

[6] Ivanov O, Yaprintsev M, Lyubushkin R, Soklakova O. Enhancement of thermoelectric efficiency in Bi2Te3 via rare earth element doping. Scripta Materialia. 2018 Mar 15;146:91-4. https://doi.org/10.1016/j.scriptamat.2017.11.031

[7] Wu F, Song H, Jia J, Hu X. Effects of Ce, Y, and Sm doping on the thermoelectric properties of Bi2Te3 alloy. Progress in Natural Science: Materials International. 2013 Aug 1;23(4):408-12. https://doi.org/10.1016/j.pnsc.2013.06.007

[8] Ismailov FI, Aliyev II. The influence of element Pr and Nd on Physico-chemical properties of solid solutions (Bi2Sb5Se3Te6I3) of n-types. InConference Intern. Proceeding Technical and Physical problems of Power Engineering. Tabriz, Iran 2010 Sep 14 (pp. 14-16).

[9] Vasil'ev A, Yaprintsev M, Ivanov O, Danshina E. Anisotropic thermoelectric properties of Bi1. 9Lu0. 1Te2. 7Se0. 3 textured via spark plasma sintering. Solid State Sciences. 2018 Oct 1;84:28-43. https://doi.org/10.1016/j.solidstatesciences.2018.08.004

[10] Vasil'ev AE, Yapryntsev MN, Ivanov ON, Zhezhu MV. Thermoelectric properties of $Bi_{2-x}Lu_xTe_{2.7}Se_{0.3}$ solid solutions. Semiconductors. 2019;53(5):657-61. https://doi.org/10.21883/ftp.2019.05.47562.20

[11] Yang J, Wu F, Zhu Z, Yao L, Song H, Hu X. Thermoelectrical properties of lutetium-doped Bi2Te3 bulk samples prepared from flower-like nanopowders. Journal of Alloys and Compounds. 2015 Jan 15;619:401-5. https://doi.org/10.1016/j.jallcom.2014.09.024

Research Article

Dielectric Stabilization and Loss Suppression in LDPE-Bi_2Te_3 Composites via Al_2O_3-Coated Aluminum Fillers

Aysel Y. Hamzayeva

Ganja State University, 429 Heydar Aliyev Avenue, AZ2001 Ganja, Azerbaijan

Received: 27.04.2026 Accepted: 26.05.2026 Published: 29.05.2026

https://doi.org/10.54414/IDIH6202

Abstract

This study investigates the dielectric properties of low-density polyethylene (LDPE)-based composite materials containing semiconducting Bi_2Te_3 and Al_2O_3-coated aluminum particles over the temperature range 20–140 °C at a constant frequency of 1 kHz. Composites containing 3 and 5 vol.% Bi_2Te_3, as well as hybrid systems incorporating Al_2O_3-coated aluminum particles (LDPE + 3% Bi_2Te_3 + 7% Al_2O_3-coated Al and LDPE + 5% Bi_2Te_3 + 5% Al_2O_3-coated Al), were analyzed. The dependencies of the dielectric permittivity (ε′) and dielectric loss tangent (tan δ) on temperature show the presence of significant stabilization of the dielectric properties, suppression of loss processes, and a decrease in temperature-induced conductivity due to the addition of Al_2O_3-coated aluminum particles. In particular, the addition of Al_2O_3-coated aluminum particles resulted in a reduction of the dielectric loss tangent by about 60–75% relative to the LDPE-Bi_2Te_3 composites containing uncoated particles, while maintaining nearly the same dielectric permittivity values. The achieved results prove that Al_2O_3 coating serves as an effective insulation layer and charge stabilization phase for LDPE-Bi_2Te_3 composites, whereas the aluminum core contributes to the enhancement of local polarization effects.

Keywords: LDPE, polymer composites, Bi_2Te_3, aluminum oxide-coated aluminum particles, dielectric permittivity, dielectric losses, interfacial polarization, electret materials

1. Introduction

In recent years, polymer composite materials have gained significant popularity in the field of dielectrics and electrets due to high electrical insulation properties and the ability to accumulate electric charge [1], [2]. One of the most commonly used polymers in this regard is low-density polyethylene (LDPE), since it demonstrates chemical stability, low dielectric losses, and electret properties [3]. Nevertheless, the rather low value of the dielectric permittivity of LDPE hinders the use of this material in the fabrication of advanced dielectric materials.

Previous studies have extensively investigated the dielectric properties of LDPE-Bi_2Te_3 composite systems [4], [5], [6]. These investigations confirmed that inclusion of semiconducting filler Bi_2Te_3 into the LDPE matrix results in an increase in dielectric permittivity of such composites due to the presence of interface polarizations. However, this increase is usually followed by a significant rise in dielectric losses and temperature dependence, thus restricting the practical applications of such materials in insulators and electrets [5], [6].

Herein, it is proposed that the use of Al particles coated with an aluminum oxide layer in the LDPE-Bi_2Te_3 composite will enable the achievement of qualitatively new levels of dielectric stabilization, rather than merely another modification of the previously reported behavior. As has been reported in other cases, ceramic oxides stabilize the dielectric response and reduce leakage currents in polymer-based materials through the insulating layer formation [7], [8], [9]. In the current case, such a stabilizing role should also be performed by the Al_2O_3 layer, which not only acts as a barrier, preventing charge transfer, but also provides deep traps in the vicinity of the polymer-semiconductor-metal/oxide interfaces [10], [11], [12].

The proposed mechanisms for stabilization are as follows:

As the first mechanism, it is assumed that Al_2O_3 layers on Al particles will act as effective insulators that will block charge transfer channels among the Bi_2Te_3 particles, reducing leakage currents and temperature-induced conduction [8], [9], [10], [11].

Secondly, the existence of the Al_2O_3 shell around the aluminum particles will induce more interfaces and deep trap centers between the polymer, semiconductor, and metal or oxide contacts. This is predicted to limit charge carrier migration and, therefore, ensure the stability of the charge trapped by the composite structure [1], [10], [12].

Third, the coating of the aluminum particles with the Al_2O_3 shell is postulated to enable an even distribution of electric field lines across the composite structure. This is predicted to limit the effect of electric field localization at the Bi_2Te_3-LDPE interfaces, and, therefore, reduce the risk of localized overheating and charge accumulation that would otherwise cause dielectric losses in the composite structure [7], [8], [9].

It can be inferred that the combination of Bi_2Te_3 and Al nanoparticles with an Al_2O_3 shell would lead to synergistic effects, where Bi_2Te_3 will provide improved dielectric properties via interfacial polarization, whereas the nonconductive Al_2O_3 shell will counteract the negative impact of semiconductor filler materials on dielectric losses and temperature dependency [8], [9], [10], [11], [12]. It is the main purpose of the current research to verify these assumptions experimentally and assess the properties of the novel composite systems. In addition, the formation of polymer-semiconductor-oxide interfaces promotes Maxwell–Wagner–Sillars interfacial polarization, which contributes to charge trapping and redistribution under an external electric field. As a result, dielectric stability is enhanced while dielectric losses are effectively suppressed.

2. Materials and Methods

2.1. Materials

LDPE (density = 0.920 g/cm^3; MFI = 2.0 g/10 min, Sigma-Aldrich) was selected as the polymer matrix because of its favorable electrical insulation property, chemical stability, and ability to form an electret. Bi_2Te_3 powder (particle size range = 10–50 µm; purity = ≥ 99.5%, Alfa Aesar) was used as a semiconductive material as a functional filler to improve interfacial polarization.

Aluminum particles coated with a native aluminum oxide (Al_2O_3) insulating layer (particle size 30–70 µm, Al_2O_3 shell thickness approximately 3–5 nm, Sigma-Aldrich) were used as an additional functional phase to stabilize the dielectric response and suppress charge transport processes within the composite.

The hybrid filler system was designed in order to combine the polarization enhancement provided by the semiconducting Bi_2Te_3 phase with the insulating and charge-stabilizing role of the Al_2O_3 shell surrounding the aluminum particles. This core-shell configuration is expected to introduce additional interfacial regions and deep charge trapping centers, which significantly influence the dielectric response of the composite.

2.2. Composite Preparation

Polymer composites were prepared by melt mixing of the fillers into the LDPE matrix using a laboratory twin-screw extruder (mixing temperature 160 °C, screw speed 60 rpm, mixing time 10 min). The required amounts of Bi_2Te_3 and Al_2O_3-coated aluminum particles were first pre-mixed mechanically and then compounded with LDPE to obtain homogeneous composite systems. Mechanical premixing was performed for approximately 20 min in order to improve filler dispersion and minimize particle agglomeration before melt processing. Two LDPE-Bi_2Te_3 compositions containing 3% and 5% Bi_2Te_3 were prepared. In addition, hybrid composite systems incorporating Al_2O_3-coated aluminum particles were fabricated with the following compositions:

- LDPE + 3% Bi_2Te_3 + 7% Al_2O_3-coated Al
- LDPE + 5% Bi_2Te_3 + 5% Al_2O_3-coated Al

After melt mixing, the composite blends were hot-pressed at 170 °C under a pressure of 10 MPa for 5 min to form disk-shaped specimens (diameter 25 mm, thickness approximately 0.5 mm) suitable for dielectric measurements. All specimens were cooled to room temperature under ambient conditions prior to measurements. The reproducibility of the preparation process was verified by fabricating several samples under identical technological conditions.

2.3. Dielectric Measurements

The dielectric properties of the prepared composites were investigated by measuring the dielectric permittivity (ε′) and dielectric loss tangent (tan δ) as a function of temperature using an Agilent 4284 A precision LCR meter equipped with a temperature-controlled measurement cell. The measurements were carried out at a fixed frequency of 1 kHz over a temperature range from 20 °C to 140 °C with a heating rate of 2 °C/min.

Prior to each measurement, gold electrodes (diameter 20 mm) were sputtered onto both surfaces of the disk-shaped specimens to ensure good electrical contact. The temperature dependences of the dielectric parameters were recorded in order to evaluate thermally activated polarization and charge transport processes in the composites. All measurements were performed under identical experimental conditions for all samples to ensure reliable comparison of the dielectric behavior between the different composite systems.

Each measurement was repeated at least three times, and the averaged values were used for the analysis. The experimental uncertainty of the dielectric parameters did not exceed ± 3%.

3. Results and Discussion

Figure 1 presents the temperature dependences of (a) the dielectric permittivity ε′ and (b) the dielectric loss tangent tan δ for LDPE-Bi_2Te_3 composites with and without the incorporation of aluminum particles coated with an Al_2O_3 insulating shell.

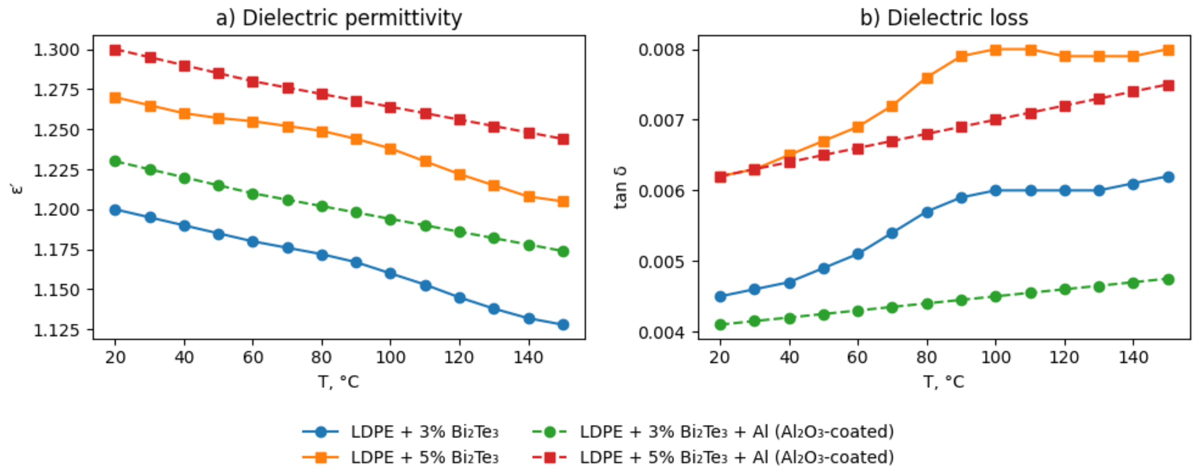

Figure 1. Temperature dependences of dielectric permittivity (ε′) and dielectric loss tangent (tan δ) for LDPE-Bi_2Te_3 and LDPE-Bi_2Te_3-Al_2O_3 composites measured at 1 kHz over the temperature range 20–140 °C.

For LDPE-Bi_2Te_3 composites without the Al_2O_3-coated aluminum particles, ε′ decreases monotonically with increasing temperature, while a higher Bi_2Te_3 content leads to systematically higher permittivity values due to enhanced interfacial polarization effects [4]. Specifically, at room temperature (20 °C), the dielectric permittivity of LDPE + 3% Bi_2Te_3 was measured as ε′ ≈ 3.8, whereas for LDPE + 5% Bi_2Te_3 it increased to ε′ ≈ 4.5. However, this enhancement is accompanied by increased dielectric losses: the tan δ values for these composites reached approximately 0.035 and 0.055, respectively, at 80 °C, and exhibited a pronounced increase at elevated temperatures due to thermally activated conductivity [5], [6].

The introduction of Al_2O_3-coated aluminum particles significantly modifies the dielectric behavior described above. Compared with the uncoated LDPE-Bi_2Te_3 composites, the systems containing Al_2O_3-coated aluminum particles exhibit significantly lower temperature sensitivity of dielectric losses, indicating suppression of conductive pathways between neighboring semiconducting particles. For example, in the case of LDPE + 3% Bi_2Te_3 + 7% Al_2O_3-coated Al samples, the value of the dielectric permittivity at 20 °C reached approximately ε' = 4.2, while the loss tangent at 80 °C was decreased to about 0.012, which is about 65% lower than in the case of the sample without Al_2O_3-coated aluminum particles (LDPE + 3% Bi_2Te_3). The same tendency was observed in LDPE + 5% Bi_2Te_3 + 5% Al_2O_3-coated Al samples, where ε' = 4.8 at 20 °C, and tan δ at 80 °C = 0.014.

It is seen that the presence of the Al_2O_3 insulating shell around the aluminum particles significantly reduces the temperature activation of charge-carrier transport and the conduction through paths connecting Bi_2Te_3 grains [8], [9], [10], [11]. The decrease in tan δ can be explained by the creation of deep energy traps at the semiconductor-polymer interfaces and the subsequent difficulty in the release and motion of charge carriers [10], [12]. This behavior is additionally associated with stabilization of interfacial polarization processes at elevated temperatures due to the insulating effect of the Al_2O_3 shell.

The observed dielectric stabilization originates from the combined contribution of enhanced interfacial polarization and restriction of thermally activated charge carrier transport. The concurrent stability of ε′ and decreasing values of tan δ imply that the dielectric properties of LDPE-Bi_2Te_3 composites with Al_2O_3-coated aluminum particles are controlled predominantly by interfacial polarization effects rather than by conductive relaxation processes. It should also be mentioned that the Al_2O_3 layer improves the homogeneity of the electric field inside the composite, thus preventing premature degradation of the composite caused by localized fields.

Such dielectric stabilization is particularly important for long-term electret applications requiring stable charge retention and low dielectric losses.

4. Conclusion

Dielectric behavior of LDPE composites incorporating Bi_2Te_3 and aluminum nanoparticles encapsulated by an insulating layer of Al_2O_3 was studied in the temperature range of 20–140 °C at a frequency of 1 kHz. Even though the LDPE-Bi_2Te_3 system provides an increase in the dielectric constant caused by interfacial polarization effects, this positive property is also associated with high dielectric losses (tan δ of up to 0.055 at 80 °C for 5% Bi_2Te_3 content).

The incorporation of Al_2O_3-coated aluminum particles significantly improves dielectric stabilization behavior, which suppresses leakage currents, reduces dielectric losses by 60–75%, and stabilizes the temperature-dependent dielectric response. The obtained results confirm the important role of interface engineering in controlling dielectric response and charge transport processes in polymer-based composite systems.

The results demonstrate that the Al_2O_3 shell plays an important insulating and charge-stabilizing role in LDPE-Bi_2Te_3 composites, contributing to reduced dielectric losses and improved dielectric stability. As a result, LDPE-Bi_2Te_3-Al_2O_3 composites emerge as promising functional materials for advanced dielectric and electret applications requiring high stability and long-term performance.

Future studies should extend the dielectric characterization to a wider frequency range (10 Hz–1 MHz) to elucidate the frequency-dependent relaxation mechanisms and further optimize the filler composition for practical electret device applications. The developed composite materials may be considered promising candidates for electret devices, dielectric insulation systems, temperature-stable capacitive elements, and charge-storage applications.

Author Contributions

The author solely contributed to the conception and design of the study, literature review, data collection, analysis and interpretation of the results, manuscript preparation, revision, and approval of the final version of the manuscript.

Conflict of Interest

The author declares no conflicts of interest.

Funding

This research received no external funding.

Acknowledgment

The author gratefully acknowledges the support provided by their institution during the course of this research.

Abbreviations

Bismuth Telluride (Bi_2Te_3), Low-Density Polyethylene (LDPE), Aluminum Oxide (Al_2O_3).

References

[1] Gerhard-Multhaupt R. Less can be more. Holes in polymers lead to a new paradigm of piezoelectric materials for electret transducers. IEEE Transactions on Dielectrics and Electrical Insulation. 2002 Dec 10;9(5):850-9. https://doi.org/10.1109/tdei.2002.1038668

[2] Lewis TJ. Interfaces are the dominant feature of dielectrics at the nanometric level. IEEE transactions on dielectrics and electrical insulation. 2004 Oct 31;11(5):739-53. https://doi.org/10.1109/tdei.2004.1349779

[3] Dang ZM, Yuan JK, Zha JW, Zhou T, Li ST, Hu GH. Fundamentals, processes and applications of high-permittivity polymer–matrix composites. Progress in materials science. 2012 May 1;57(4):660-723. https://doi.org/10.1016/j.pmatsci.2011.08.001

[4] Zhang G, Allahyarov E, Zhu L. Polymer nanodielectrics: current accomplishments and future challenges for electric energy storage. InNano/Micro-Structured Materials for Energy and Biomedical Applications: Latest Developments, Challenges and Future Directions 2018 Feb 9 (pp. 1-48). Singapore: Springer Singapore. https://doi.org/10.1007/978-981-10-7787-6_1

[5] Dang ZM, Yuan JK, Zha JW, Zhou T, Li ST, Hu GH. Fundamentals, processes and applications of high-permittivity polymer–matrix composites. Progress in materials science. 2012 May 1;57(4):660-723. https://doi.org/10.1016/j.pmatsci.2011.08.001

[6] Luo H, Zhou X, Ellingford C, Zhang Y, Chen S, Zhou K, Zhang D, Bowen CR, Wan C. Interface design for high energy density polymer nanocomposites. Chemical Society Reviews. 2019;48(16):4424-65. https://doi.org/10.1039/c9cs00043g

[7] Zhang X, Shen Y, Xu B, Zhang Q, Gu L, Jiang J, Ma J, Lin Y, Nan CW. Giant Energy Density and Improved Discharge Efficiency of Solution-Processed Polymer Nanocomposites for Dielectric Energy Storage. Advanced materials (Deerfield Beach, Fla.). 2016 Jan 14;28(10):2055-61. https://doi.org/10.1002/adma.201503881

[8] Zhou T, Zha JW, Hou Y, Wang D, Zhao J, Dang ZM. Surface-functionalized MWNTs with emeraldine base: preparation and improving dielectric properties of polymer nanocomposites. ACS Applied Materials & Interfaces. 2011 Dec 28;3(12):4557-60. https://doi.org/10.1021/am201454e

[9] Li JY, Zhang L, Ducharme S. Electric energy density of dielectric nanocomposites. Applied physics letters. 2007 Mar 26;90(13). https://doi.org/10.1063/1.2716847

[10] Xu J, Wong CP. Low-loss percolative dielectric composite. Applied Physics Letters. 2005 Aug 22;87(8). https://doi.org/10.1063/1.2032597

[11] Dang Z.-M, Zheng MS, Zha JW. 1D/2D carbon nanomaterial-polymer dielectric composites with high permittivity for power energy storage applications. Small. 2016 Apr;12(13):1688-701. https://doi.org/10.1002/smll.201503193

[12] Zhang C, Shi Z, Mao F, Yang C, Yang J, Zhu X, Zuo H. Polymer composites with balanced dielectric constant and loss via constructing trilayer architecture. Journal of Materials Science. 2018 Sep;53(18):13230-42. https://doi.org/10.1007/s10853-018-2545-4

[13] Luo H, Zhou X, Ellingford C, Zhang Y, Chen S, Zhou K, Zhang D, Bowen CR, Wan C. Interface design for high energy density polymer nanocomposites. Chemical Society Reviews. 2019;48(16):4424-65. https://doi.org/10.1039/c9cs00043g

[14] Li Q, Chen L, Gadinski MR, Zhang S, Zhang G, Li HU, Iagodkine E, Haque A, Chen LQ, Jackson TN, Wang Q. Flexible high-temperature dielectric materials from polymer nanocomposites. Nature. 2015 Jul 30;523(7562):576-9. https://doi.org/10.1038/nature14647

[15] Prateek, Thakur VK, Gupta RK. Recent progress on ferroelectric polymer-based nanocomposites for high energy density capacitors: synthesis, dielectric properties, and future aspects. Chemical reviews. 2016 Apr 13;116(7):4260-317. https://doi.org/10.1021/acs.chemrev.5b00495

[16] Chi Q, Ma T, Zhang Y, Chen Q, Zhang C, Cui Y, Zhang T, Lin J, Wang X, Lei Q. Excellent energy storage of sandwich-structured PVDF-based composite at low electric field by introduction of the hybrid CoFe2O4@ BZT–BCT Nanofibers. ACS Sustainable Chemistry & Engineering. 2018 Jan 2;6(1):403-12. https://doi.org/10.1021/acssuschemeng.7b02659

Journal of Nanotechnology and Innovative Materials

Review Article

Nanosensor Technologies and Artificial Intelligence-Based Optimization Methods in Quantum Computing

Gulnar A. Hamidova[1] and Ulfat R. Mirzayev[1]

[1]Department of Mechanics and Mathematics, School of Advanced Technologies and Innovation Engineering, Western Caspian University, Ahmad Rajabli 17A, III Parallel, AZ1001 Baku, Azerbaijan

Received: 06.04.2026 Accepted: 18.05.2026 Published: 29.05.2026

https://doi.org/10.54414/IHMO3856

Abstract

The rapid development of modern information technologies provides for the creation of systems with higher computing power. Traditional computer systems are widely used to solve computational problems involving the processing of large and complex datasets. Owing to their enormous computational potential, quantum computers have become a major focus of scientific research. However, the practical implementation of quantum systems remains a significant challenge. External environmental factors, electromagnetic effects, temperature changes, and quantum decoherence can reduce the productivity of the system. Nanosensor technologies combined with artificial intelligence-based optimization methods provide promising solutions to these challenges. Nanosensors enable highly sensitive monitoring of environmental conditions surrounding quantum hardware. Artificial intelligence technologies analyze system behavior to reduce errors and improve performance. In this work, the application areas, advantages, and future development prospects of nanosensor technologies and artificial intelligence-based optimization methods in quantum computers are investigated.

Keywords: Quantum computers, nanosensor, artificial intelligence, qubit, machine learning, optimization

1. Introduction

In the modern information society, the volume of data and the speed of its processing are rapidly increasing. Traditional computer systems have been the main tool for solving various computational problems for many years. However, with the development of technology, the volume of complex calculations has also increased, and the limitations of classical computer systems have become more noticeable.

In order to overcome these limitations, the idea of creating quantum computers arose. Quantum computers operate based on the fundamental laws of quantum mechanics and differ significantly from classical computers. While the bits used in traditional computers can only be in the 0 or 1 state, the qubits used in quantum computers can exist in both the 0 and 1 states at the same time [1].

While quantum computing offers undeniable benefits, deploying this technology in practical scenarios presents significant hurdles. A primary obstacle lies in preserving qubit stability and shielding them from environmental disruptions, as even minor external fluctuations can significantly compromise system performance [2], [3]. To tackle these issues, recent advancements have increasingly relied on the integration of nanotechnology and artificial intelligence. Specifically, nanosensors enable precise tracking of the quantum state, while AI algorithms optimize system operations to drastically reduce error rates.

2. The Working Principle of Quantum Computers

Operating on the foundational laws of quantum mechanics, quantum computers utilize the qubit as their primary computing unit [1], [4]. The defining characteristic of qubits is their capacity to leverage the core principles of both superposition and quantum entanglement [5].

Superposition means that quantum particles can exist in several states at the same time [1]. This feature significantly increases computing capabilities. For example, while two bits in a classical computer can only be in one state, two qubits can exist in a superposition of four computational basis states simultaneously.

Another important feature is quantum entanglement. In quantum entanglement, a special connection is created between two or more qubits, and measurements performed on one entangled qubit produce correlations with its entangled partner that cannot be explained classically. This feature ensures the implementation of parallel calculations [1].

However, various problems arise during the operation of quantum computers. One of them is decoherence. Decoherence is a process that occurs due to external environmental influences and leads to the destruction of quantum states [2]. The main factors affecting the operation of qubits are shown in Figure 1.

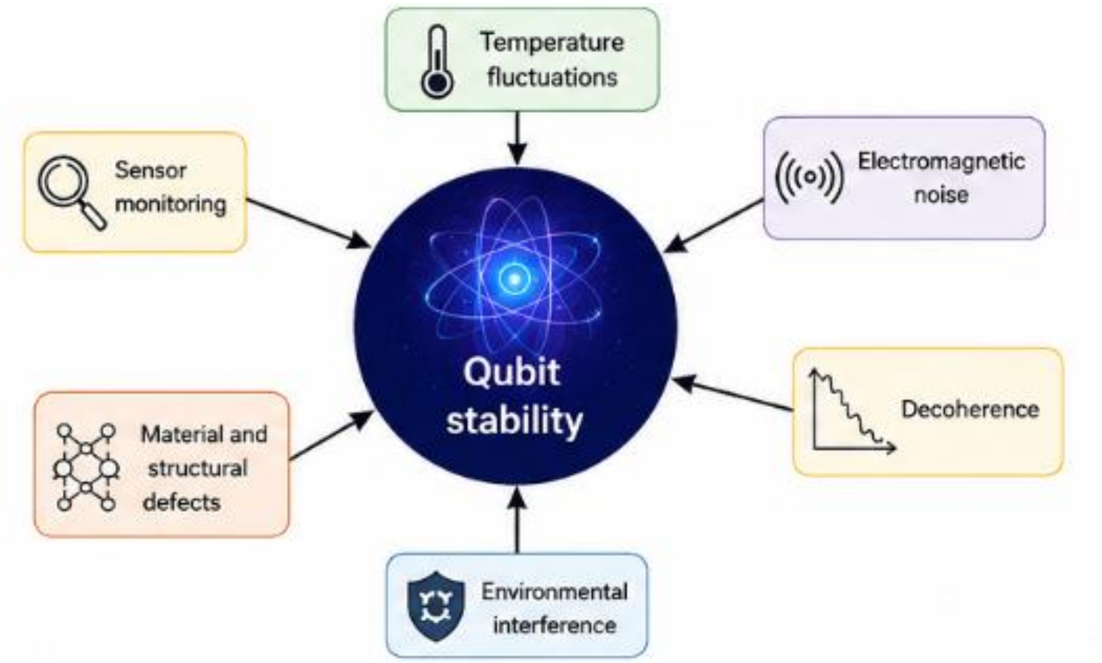

Figure 1. Environmental factors affecting qubit stability.
Source: Author's own elaboration based on [1].

3. Application of Nanosensor Technologies in Quantum Computers

Advances in nanotechnology have enabled the development of highly sensitive nanoscale sensors [6]. Nanosensors have very small dimensions and can operate with high sensitivity.

The main areas of application of nanosensors in quantum computers are as follows:

- Monitoring temperature changes;
- Measuring electromagnetic effects;
- Monitoring qubit states;
- Ensuring system stability;
- Collecting data in real time.

The operation of quantum computers is highly dependent on environmental conditions. Even a slight temperature change can affect the operation of the system. Nanosensors can immediately detect these changes [6]. The interaction of nanosensor technologies and an artificial intelligence-based control system is shown in Figure 2.

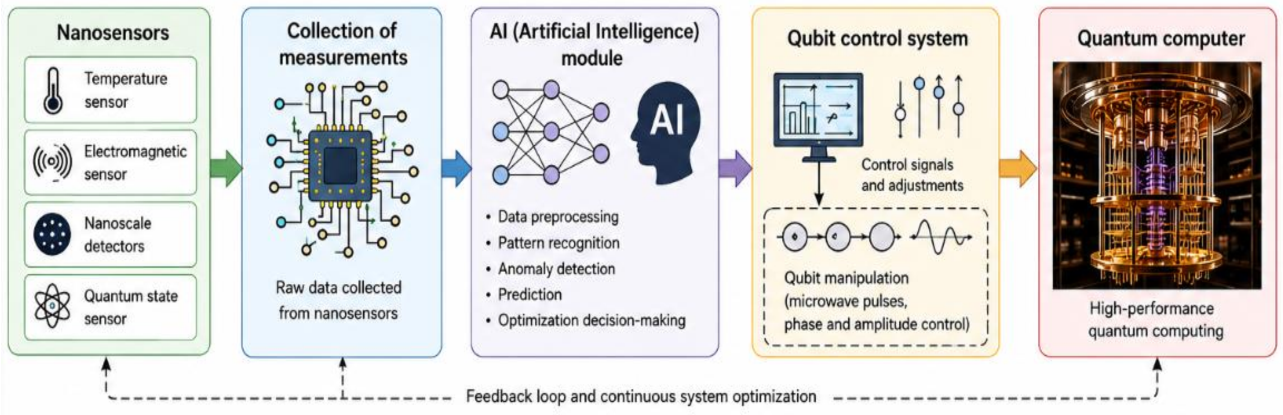

Figure 2. Architecture of a nanosensor and AI-based control system for quantum computers.
Source: Author's own elaboration.

In addition, nanosensors also detect electromagnetic effects. Since quantum systems are very sensitive, external electromagnetic signals can negatively affect their operation [6], [7]. Based on the information received from the sensors, it is possible to eliminate problems in time.

The application of nanosensors can also help create large-scale quantum systems. As the number of qubits increases, the control of the systems becomes more complex. Continuous sensor-based data acquisition simplifies system monitoring and control.

4. Artificial Intelligence-Based Optimization Methods

Artificial intelligence technologies have been widely applied in various fields over the past decade. Artificial intelligence systems also play an important role in the field of quantum computers. Machine learning algorithms can analyze large volumes of data obtained from quantum systems [8], [9], [10], [11]. As a result of these analyses, various problems can be identified in advance. The process of data processing and optimization in quantum systems of artificial intelligence is presented in Figure 3.

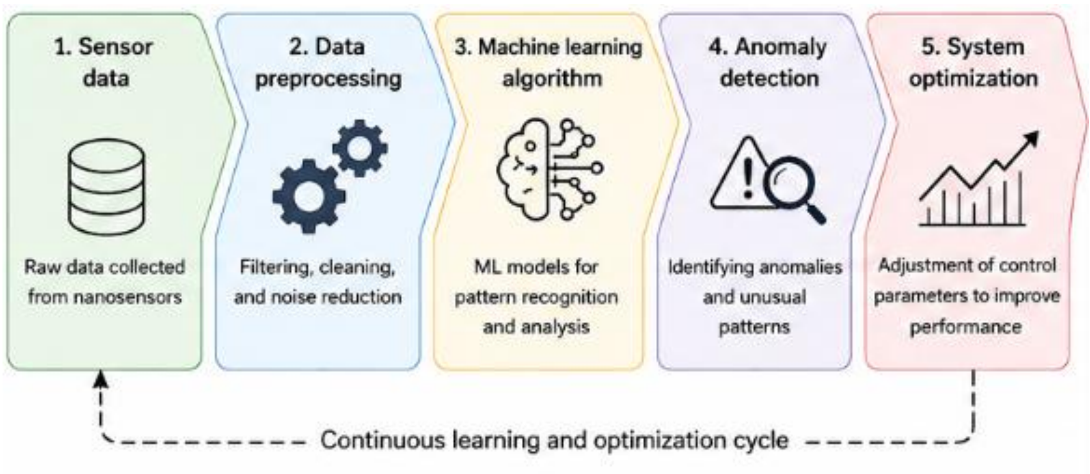

Figure 3. Artificial intelligence-based optimization workflow in quantum systems.
Source: Developed by the authors based on [8], [9], [10], [11].

One of the artificial intelligence-based methods is the error detection system. The main cause of errors in quantum computers is noise and decoherence. Artificial intelligence models help to prevent them by analyzing these errors [12]. Another important method is the use of neural networks. Neural networks can learn system behavior and predict future changes [9]. Reinforcement learning is also used in quantum optimization [10]. Through this method, the system improves its performance based on experience and makes more optimal decisions. Artificial intelligence (AI) also enables predictive maintenance of quantum systems. Predictive analytics enables the early detection of equipment failures.

5. Integration of Nanosensor Technologies and Artificial Intelligence

The combined use of nanosensors and artificial intelligence technologies creates new opportunities in the development of quantum computers.

Nanosensors collect data in real time, and artificial intelligence systems process this data. Based on data analysis, artificial intelligence systems can make adaptive decisions to optimize system performance.

The main advantages of this integration are as follows:

• Increasing calculation accuracy;
• Minimizing errors;
• Improving system stability;
• Efficient use of resources;
• Facilitating the management of large-scale systems.

Future advancements in these technologies are expected to enable the development of more powerful and reliable quantum computing systems.

6. Intelligent Quantum Stability Framework

One of the major limitations preventing the large-scale implementation of quantum computers is the instability of qubits and their sensitivity to external environmental factors. Although existing studies discuss the use of nanosensors and artificial intelligence separately, there are still limited studies proposing an integrated framework that combines both technologies in a unified architecture. Therefore, this research proposes a new conceptual model called the Intelligent Quantum Stability Framework (IQSF).

The proposed framework is based on the continuous interaction between nanosensor technologies and artificial intelligence algorithms. In this architecture, nanosensors are responsible for collecting real-time information about the operating environment of quantum computers. The collected data include temperature fluctuations, electromagnetic interference, vibrations, humidity levels, and various noise parameters that directly affect qubit stability.

After the data are collected, they are transferred to an artificial intelligence module. Machine learning algorithms process these data and identify hidden relationships between environmental factors and the behavior of qubits. Unlike traditional monitoring systems, the proposed framework not only detects existing errors but also predicts potential system failures before they occur.

The predictive capability of the framework is based on neural network algorithms. The neural network is trained using historical data obtained from nanosensors and continuously updates its parameters as new information becomes available. Consequently, the system can determine the probability of decoherence and estimate the likelihood of computational errors in advance.

Another important component of the IQSF model is its automatic decision-making mechanism. Once the artificial intelligence system predicts an abnormal condition, it immediately generates corrective actions [8], [9]. These actions may include reducing the computational load, activating electromagnetic shielding mechanisms, adjusting cooling systems, or initiating quantum error correction protocols.

The proposed framework consists of five major stages:

1. Real-time environmental monitoring using nanosensors;
2. Data transmission and storage;
3. Artificial intelligence-based data analysis;
4. Prediction of decoherence and system errors;
5. Automatic correction and stabilization of quantum operations.

The integration of these stages creates a self-adaptive quantum computing environment. Unlike conventional monitoring approaches, the proposed system continuously learns from previous experiences and improves its prediction accuracy over time.

The implementation of the IQSF architecture can provide several important advantages. First, it can significantly reduce the probability of qubit decoherence. Second, it improves the stability and reliability of quantum computations. Third, it decreases maintenance costs by identifying failures before they become critical. Finally, it enables the development of scalable quantum systems with a large number of qubits.

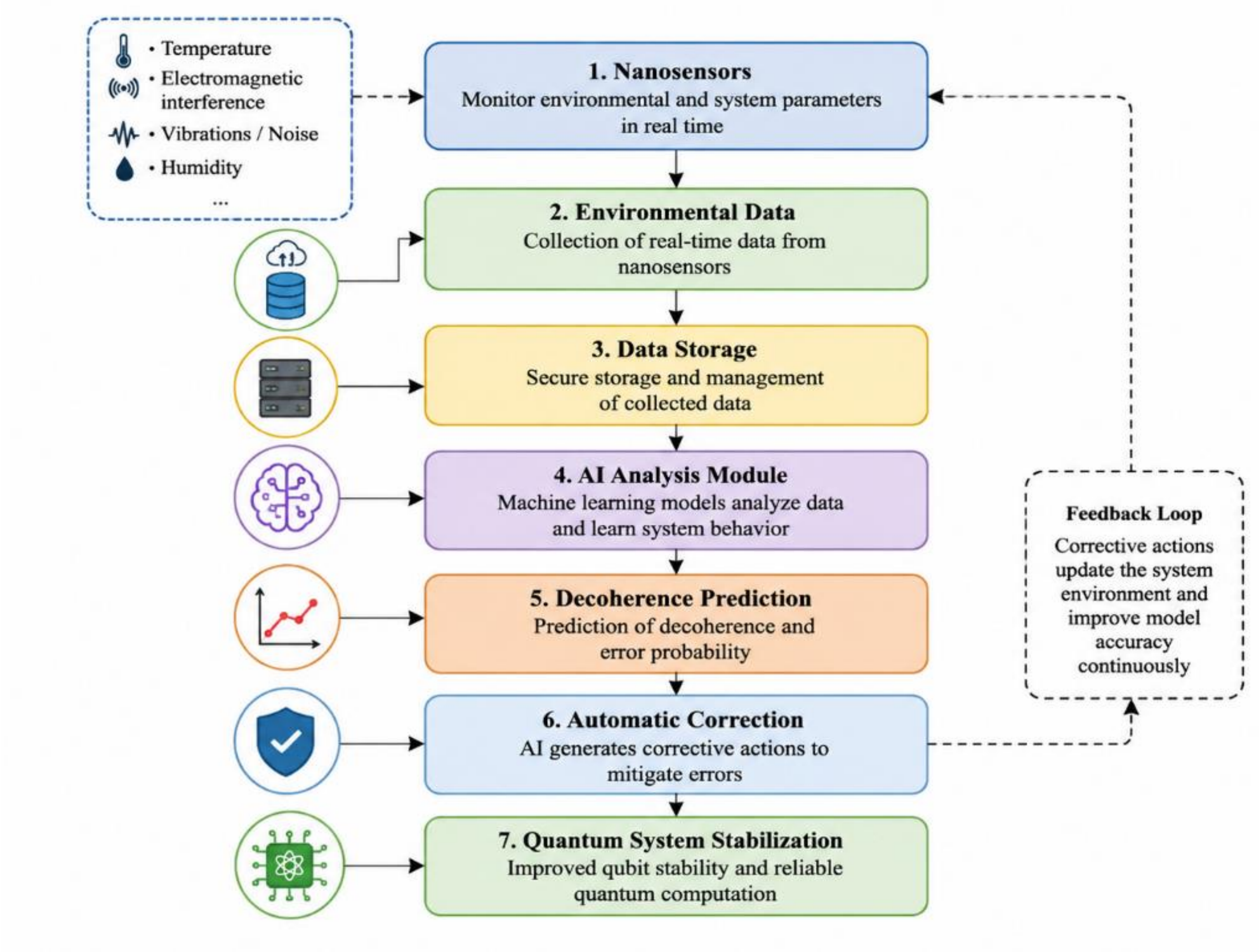

Figure 4. Intelligent Quantum Stability Framework (IQSF).
Source: Author's own elaboration.

To evaluate the efficiency of the proposed framework, this study introduces the concept of the Quantum Stability Index (QSI). The index represents the relationship between environmental disturbances and the overall stability of a quantum system and can be expressed as:

$$QSI = \alpha T + \beta E + \gamma N + D$$

where:

- QSI – Quantum Stability Index;
- T – Temperature variation;
- E – Electromagnetic interference;
- N – Noise level;
- D – Decoherence coefficient;
- α, β and γ – weighting coefficients.

The following equation is proposed as a conceptual indicator rather than a validated mathematical model.

A lower value of the index indicates a more stable quantum environment, whereas higher values indicate an increased probability of computational errors and qubit instability.

The proposed IQSF model can serve as a theoretical basis for future experimental studies and may contribute to the development of next-generation intelligent quantum computing systems. Future research may involve the practical implementation of this framework using real nanosensor devices and deep reinforcement learning algorithms for autonomous quantum optimization.

7. Conclusion

Current research highlights quantum computing as a cornerstone of next-generation information technology, with the potential to trigger revolutionary shifts across scientific research, industrial operations, finance, healthcare, and cybersecurity [13], [14]. Unlike conventional computers, which struggle with large-scale, complex computational bottlenecks, quantum systems leverage quantum mechanical phenomena to achieve vastly superior processing power.

Nevertheless, transitioning these systems into practical deployment is hindered by major hurdles, specifically in maintaining qubit stability, suppressing system noise, and mitigating computational errors. Findings indicate that nanosensing technologies are pivotal in supervising quantum environments. Thanks to their extreme sensitivity, nanosensors capture precise metrics regarding thermal shifts, electromagnetic interference, and other ambient disturbances. Gathering this data continuously allows for the immediate identification of system deviations and the preemptive detection of vulnerabilities, thereby fostering a more stable and resilient quantum infrastructure.

In addition to the theoretical analysis presented in this study, a novel Intelligent Quantum Stability Framework (IQSF) has been proposed to improve the reliability and stability of quantum computing systems. The proposed framework integrates nanosensor technologies with artificial intelligence methods to enable real-time monitoring, prediction of decoherence, and automatic error correction. This conceptual model may serve as a basis for future experimental research and contribute to the development of more stable, scalable, and efficient quantum computer architectures.

Concurrently, optimization frameworks driven by artificial intelligence are essential for maximizing quantum efficiency [8], [9]. Utilizing machine learning and neural networks enables the sophisticated analysis of data streams generated by quantum hardware. These AI models are capable of diagnosing systematic errors, forecasting future behavior, and executing automated corrective actions. Consequently, these methodologies drastically lower error rates while significantly enhancing overall computational precision.

Author Contributions

Both authors contributed to the conceptualization, literature review, writing, revision, and editing of the manuscript. Both authors have read and approved the final version of the manuscript.

Conflict of Interest

The authors declare no conflicts of interest.

Funding

This research received no external funding.

Acknowledgment

The authors would like to thank Western Caspian University for its continuous academic support.

Abbreviations

Intelligent Quantum Stability Framework (IQSF), Quantum Stability Index (QSI), Artificial intelligence (AI).

References

[1] Nielsen MA, Chuang IL. Quantum computation and quantum information. Cambridge university press; 2010 Dec 9.

[2] Terhal BM. Quantum error correction for quantum memories. Reviews of Modern Physics. 2015 Apr 1;87(2):307-46. https://doi.org/10.1103/revmodphys.87.307
[3] Preskill J. Quantum computing in the NISQ era and beyond. Quantum. 2018 Aug 6;2:79. https://doi.org/10.22331/q-2018-08-06-79
[4] DiVincenzo DP. The physical implementation of quantum computation. Fortschritte der Physik: Progress of Physics. 2000 Sep;48(9-11):771-83. https://doi.org/10.1002/1521-3978(200009)48:9/11%3C771::aid-prop771%3E3.0.co;2-e
[5] Krantz P, Kjaergaard M, Yan F, Orlando TP, Gustavsson S, Oliver WD. A quantum engineer's guide to superconducting qubits. Applied physics reviews. 2019 Jun 1;6(2). https://doi.org/10.1063/1.5089550
[6] Degen CL, Reinhard F, Cappellaro P. Quantum sensing. Reviews of modern physics. 2017 Jul 1;89(3):035002. https://doi.org/10.1103/revmodphys.89.035002
[7] Awschalom DD, Hanson R, Wrachtrup J, Zhou BB. Quantum technologies with optically interfaced solid-state spins. Nature Photonics. 2018 Sep;12(9):516-27. https://doi.org/10.1038/s41566-018-0232-2
[8] Shuford J. Quantum computing and artificial intelligence: synergies and challenges. Journal of Artificial Intelligence General Science (JAIGS). 2024 Jan;1(1). https://doi.org/10.60087/jaigs.v1i1.35
[9] LeCun Y, Bengio Y, Hinton G. Deep learning. nature. 2015 May 28;521(7553):436-44. https://doi.org/10.1038/nature14539
[10] Cerezo M, Verdon G, Huang HY, Cincio L, Coles PJ. Challenges and opportunities in quantum machine learning. Nature computational science. 2022 Sep;2(9):567-76. https://doi.org/10.1038/s43588-022-00311-3
[11] Biamonte J, Wittek P, Pancotti N, Rebentrost P, Wiebe N, Lloyd S. Quantum machine learning. Nature. 2017 Sep 14;549(7671):195-202. https://doi.org/10.1038/nature23474
[12] Liao H, Wang DS, Sitdikov I, Salcedo C, Seif A, Minev ZK. Machine learning for practical quantum error mitigation. Nature Machine Intelligence. 2024 Dec;6(12):1478-86. https://doi.org/10.1038/s42256-024-00927-2
[13] Bennett CH, Brassard G. Quantum cryptography: Public key distribution and coin tossing. Theoretical computer science. 2014 Dec 4;560:7-11. https://doi.org/10.1016/j.tcs.2014.05.025
[14] Pirandola S, Andersen UL, Banchi L, Berta M, Bunandar D, Colbeck R, Englund D, Gehring T, Lupo C, Ottaviani C, Pereira JL. Advances in quantum cryptography. Advances in optics and photonics. 2020 Dec 14;12(4):1012-236. https://doi.org/10.1364/aop.361502

Journal of Nanotechnology and Innovative Materials

Research Article

Creating a Term Database for Patentability Search in the Field of Nanotechnology

Alikhan I. Rzaguliev

Department of Information Technologies, School of Advanced Technologies and Innovation Engineering, Western Caspian University, Ahmad Rajabli 17A, III Parallel, AZ1001 Baku, Azerbaijan

Received: 25.04.2026 Accepted: 26.05.2026 Published: 29.05.2026

https://doi.org/10.54414/WUSO3256

Abstract

The present study examines the design of a multilingual database of technical terms that could be used in automated searches for patents in the area of nanotechnologies. Patents in the field of nanotechnology present several challenges due to terminology issues, documentation in several languages, and different terminological expressions used in science. The database suggested includes the organization of technical terminology into noun-based categories in three languages (Azerbaijani, English, and Russian) and also incorporates synonym management techniques. The study explains the use of structured vocabularies of technical terms for automated patent searching and presents the development of a multilingual database in order to aid semi-automatic patentability evaluation.

Keywords: patentability search, nanotechnologies, automation, knowledge-based systems, decision support, technical database

1. Introduction

The patentability search in the domain of nanotechnologies faces a number of difficulties associated with the specificity of technical terms, high pace of technological changes, and multilinguality of patents. Inventions related to nanotechnologies are commonly represented using certain scientific language, including scientific expressions, acronyms, and specific technical terms. Thus, the traditional keyword-based patent search may fail to identify the relevant prior-art documents if synonyms and other linguistic representations of technical terms are used.

Meanwhile, modern patent offices apply more and more automatic and semi-automatic search tools in order to increase efficiency and facilitate patent examination. Still, the success of such searches heavily depends on the structure and content of technical term databases used to generate search queries and semantic analysis. Current universal dictionaries are not always effective in relation to particular domains, e.g., nanotechnologies.

The goal of this study is to elaborate a structured multilingual technical term database for automated patentability search in the nanotechnology domain.

2. Literature Review

Currently, in the Patent and Trademark Centre under the Intellectual Property Agency of the Republic of Azerbaijan, patent search is conducted in multiple databases. In each database, the examiner conducts a manual search using Boolean Algebra operations (such as AND, OR, NOT, etc). The databases include: Azerbaijani Patent database where examiner searches in Azerbaijani and Russian [1], FIPS where the examiner searches in (mainly for Azerbaijani practice) Russian [2], EAPATIS where the examiner searches in (mainly for Azerbaijani practice) Russian [3], PATENTSCOPE where the examiner searches in (mainly for Azerbaijani practice) English [4], Espacenet where the examiner searches in (mainly for Azerbaijani practice) English [5], USPTO where the examiner searches in (mainly for Azerbaijani practice) English [6], Google Patents where the examiner searches in (mainly for Azerbaijani practice) English [7].

According to the patent law of the Republic of Azerbaijan, the subjects of patents can be inventions, utility models, and industrial designs. In the Republic of Azerbaijan, utility models can only be devices. While inventions must satisfy three patentability requirements, utility models are required to satisfy only two criteria. Those are novelty and industrial applications. The devices for novelty conditions must-have new characteristics. If the device can be made or used in any field of industry and economy, then the invention is considered applicable [8].

Unlike some other national or regional patent legislations, in the Republic of Azerbaijan, examiners also provide supplementary examinations for utility models. The publication of the utility model occurs only after the patent search. Depending on the patent search, the examiner decides whether to grant or reject the application [8].

The area of patent retrieval and automated patent searching has gained significance because of the fast expansion of patent documentation across the globe. Currently, research efforts in the field mainly concentrate on semantic similarity, natural language processing, and machine learning techniques to improve patent searching.

Another study proposes an automated patent search approach by using machine learning and NLP to compare the full texts of patents, contrary to manual keyword search. The approaches used by the authors in this study include vector-based similarity and Cosine similarity. They use two different datasets for their research: a dataset of 2.4 million cited or random pairs and an expert-annotated dataset to extract relevant documents. The authors represent documents in numeric vectors, including Bag-of-Words, word2vec, doc2vec, LSA, and KPCA [9].

Different sources describe patent information retrieval methods. Where the authors mention ways of semantic patent retrieval, transformer models, patent embeddings, etc. The authors use European Patent Office search reports as a training data sample [10].

Another study presents a model for improving search query accuracy on specialized websites using text correction and reconstruction. The authors train an intelligent model to correct user-entered queries and reconstruct them for improved retrieval results. According to the authors, the system was implemented in Go (Golang) for backend efficiency on concurrent operations. The model achieved a very high accuracy of 99.85% after 15 epochs of training, with a testing accuracy of about 88% on a validation dataset of heavily altered queries. The focus was on the query input stage of search systems for improving user query quality [11].

The article addresses the important challenge of query reconstruction for specialized retrieval systems. The paper does not cover the downstream stages of search execution, similarity scoring, multilingual input handling, or classification. Sometimes, for conducting patentability, search logic might be required. And logic-based patentability evaluation is absent in this paper. The current research differs from the existing ones because it concentrates on creating a multilingual technical term database for automated patentability analysis.

In the proposed automated patentability search system, patent retrieval is performed using a multi-step search model. Unlike the previously proposed model, which employed a binary (0–1) scoring scale, the present approach adopts a 0–10 scoring scale to provide a more intuitive interpretation of similarity scores. The three-step patent search framework is retained, while the definitions of the X and Y similarity labels are further clarified. In addition, the proposed model incorporates International Patent Classification (IPC) similarity into the overall similarity assessment. IPC similarity is evaluated on a 0–10 scale according to the hierarchical distance between IPC codes and is integrated into the similarity scoring functions (S_X and S_Y), requiring corresponding modifications to the original formulas [12].

$$S_Y = \frac{S_N + S_{noun} + S_{adj} + S_{IPC}}{4} \quad (1) \quad [12]$$

$$S_X = \frac{S_N + S_{noun} + S_{adj} + S_{IPC} + S_C}{5} \quad (2) \quad [12]$$

$$S_{IPC\ N} = CD \times 2 \quad (3) \quad [12]$$

$$S_{IPC} = IPC_1 \times IPC_{w1} + IPC_2 \times IPC_{w2} \ldots IPC_N \times IPC_{wn} \quad (4) \quad [12]$$

In Equations (3) and (4), S_{IPC} represents the similarity score of the International Patent Classification (IPC) codes. IPC similarity is determined according to the hierarchical distance between two IPC classifications. For example, the IPC code F16H 7/06 can be divided into hierarchical levels (F, F16, F16H, F16H7, and F16H7/06). The similarity score increases with the number of matching hierarchical levels, corresponding to values of 2, 4, 6, 8, and 10, respectively. For a single IPC code, $SIPC_n$ denotes the similarity score, where CD represents the number of common hierarchical levels. When multiple IPC codes are assigned to a patent, the overall IPC similarity (SIPC) is calculated as the weighted sum of the individual IPC similarity scores, where the weights satisfy the condition $w_1 + w_2 + \ldots + w_n = 1$ [12].

3. Databases

To simplify the analysis, only polymer-related nanotechnology patents were used as sample data. Sample noun and adjective keywords were selected from PATENTSCOPE with the search query "EN_TI:(Polymer AND nanotechnology)". The search returned four patent documents [13].

Sample data for configuration keywords were selected from published inventions or utility models from 2022 and onward in Azerbaijan [14].

Table 1. English noun keyword database.

Term №	Noun keyword	Term №	Noun keyword	Term №	Noun keyword
1	equipment	12	pMHC	22	D-Tartrate
2	multimer	13	modification	23	DBCO
3	DNA	14	SpyTag	24	nitride
4	Carbon	15	Emission	25	milliequiv
5	Composition	16	SpyCatcher	26	polystyrene
6	N- succinimidyl-S-acetylthiopropionate	17	glucocerebrosidase	27	oxide
7	pole	18	polycarbonates	28	carbide
8	pH	19	boride	29	polyacrylates
9	Aircraft	20	polymer	30	Isofagomine
10	polyethylene	21	alloy	31	polypropylene
11	N-succinimidyl-S-acetylthiopropionate				

Table 2. English noun adjuncts keyword database (nouns used as adjectives).

Term №	Noun ad. keyword	Term №	Noun ad. keyword	Term №	Noun ad. keyword
1	ratio	12	Drag	23	molding
2	salt	13	Flight	24	net
3	drug	14	Nanoparticle	25	C linking
4	fusion	15	clay	26	amino fluid
5	chain	16	coating	27	metal
6	capture	17	solvent	28	emulsifying
7	Surface	18	protein	29	Cream
8	Powder	19	strand	30	Liquid
9	Nanocomposite	20	molecular chaperone	31	micron
10	Agent	21	Fuel	32	plastic
11	Value	22	Injection	33	water

Table 3. English adjective keyword database.

Term №	Adj. keyword	Term №	Adj. keyword	Term №	Adj. keyword
1	PE-modified	7	insulating	13	Molar
2	rectangular	8	organic	14	polyurethane
3	magnetic	9	silanol	15	conducting
4	submicron	10	reactive	16	non-destructive
5	Invisible	11	Aprotic	17	Nanoscale

6	electrically	12	HLB

Table 4. English configuration keyword database.

Term №	Configuration keywords	Term №	Configuration keywords	Term №	Configuration keywords
1.	Installed	2.	Connected	3.	Passes through the center
2.	Mounted	4.	Opposite	6.	Fixed
3.	Settled	6.	Lined up	9.	Inclusive
4.	Placed	8.	Attached	12.	Linked

Table 5. Azerbaijani noun keyword database.

Term №	Noun keyword	Term №	Noun keyword	Term №	Noun keyword
1	avadanlıq	12	pMHC	22	D- tartrat
2	multimer	13	modifikasiya	23	DBCO
3	DNT	14	SpyTag	24	nitrid
4	Karbon	15	emissiya	25	milliekviv
5	Tərkib	16	SpyCatcher	26	polistirol
6	N- suksinimidil-S-asetiltiopropionat	17	qlükoserebrozidaza	27	oksid
7	Qütb	18	polikarbonatlar	28	karbid
8	pH	19	borid	29	poliakrilatlar
9	Təyyarə	20	polimer	30	izofagomin
10	polietilen	21	ərinti	31	polipropilen
11	N- suksinimidil-S-asetiltiopropionat				

Table 6. Azerbaijani noun adjuncts keyword database (nouns used as adjectives).

Term №	Noun ad. keyword	Term №	Noun ad. keyword	Term №	Noun ad. keyword
1	Nisbət	12	Sürükləmə	23	qəlibləmə
2	duz	13	Uçuş	24	tor
3	dərman	14	Nanohissəcik	25	C birləşdirici
4	birləşmə	15	Gil	26	amino mayesi
5	zəncir	16	Örtük	27	metal
6	tutma	17	Həlledici	28	emulsiya
7	Səth	18	zülal	29	krem
8	Toz	19	Tel	30	maye
9	Nanokompozit	20	molekulyar şaperon	31	mikron
10	Agent	21	Yanacaq	32	plastik
11	Dəyər	22	inyeksiya	33	su

Table 7. Azerbaijani adjective keyword database.

Term №	Adj. keyword	Term №	Adj. keyword	Term №	Adj. keyword
1	PE ilə modifikasiya edilmiş	7	izolyasiyaedici	13	molar
2	düzbucaqlı	8	üzvi	14	poliuretan
3	maqnit	9	silanol	15	keçirici
4	submikron	10	reaktiv	16	dağıdıcı olmaya
5	görünməz	11	aprotik	17	nanoölçü
6	elektrik	12	HLB		

Table 8. Azerbaijani configuration keyword database.

Term №	Configuration keyword	Term №	Configuration keyword	Term №	Configuration keyword
1.	Quraşdırılımış	2.	Qoşulub	3.	Mərkəzindən keçir
2.	Oturdulmuş	4.	Əks tərəf	6.	Sabitlənmiş
3.	Bərkidilmiş	6.	Düzülüb	9.	Daxil edilib
4.	Yerləşən	8.	Bitişik	12.	Birləşib

Table 9. Russian noun keyword database.

Term №	Noun keyword	Term №	Noun keyword	Term №	Noun keyword
1	оборудование	12	пМГК	22	D-тартрат
2	мультимер	13	модификация	23	DBCO
3	ДНК	14	SpyTag	24	нитрид
4	Углерод	15	эмиссия	25	миллиэквивалента
5	Состав	16	SpyCatcher	26	полистирол
6	N-сукцинимидил-S-ацетилтиопропионат	17	глюкоцереброзидаза	27	оксид
7	полюс	18	поликарбонатов	28	карбид
8	pH	19	борид	29	полиакрилатов
9	Самолет	20	полимер	30	Изофагомин
10	полиэтилен	21	сплав	31	полипропилен
11	N-сукцинимидил-S-ацетилтиопропионат				

Table 10. Russian noun adjuncts keyword database (nouns used as adjectives).

Term №	Noun ad. keyword	Term №	Noun ad. keyword	Term №	Noun ad. keyword
1	соотношение	12	Сопротивление	23	формование
2	соль	13	Полет	24	сетка
3	лекарство	14	Наночастица	25	С-связывание
4	слияние	15	глина	26	аминожидкости
5	цепь	16	покрытие	27	металл
6	захват	17	растворитель	28	эмульгирующий
7	Поверхность	18	белок	29	Крем
8	Порошок	19	нить	30	Жидкость
9	Нанокомпозит	20	молекулярный шаперон	31	микрон
10	Агент	21	Топливо	32	пластик
11	Значение	22	инъекция	33	вода

Table 11. Russian adjective keyword database.

Term №	Adj. keyword	Term №	Adj. keyword	Term №	Adj. keyword
1	ПЭ-модифицированный	7	изоляционных	13	Молярный
2	полиуретан	8	органический	14	полиуретан
3	магнитный	9	силанол	15	проводящий
4	субмикронный	10	реактивный	16	неразрушающих
5	Невидимый	11	апротонный	17	наноразмер
6	электропроводящий	12	HLB		

Table 12. Russian configuration keyword database.

Term №	Configuration keywords	Term №	Configuration keywords	Term №	Configuration keywords
1.	Установлено	2.	Подключенный	3.	Проходит через центр
2.	Поставленный	4.	Напротив	6.	Фиксированный
3.	Закреплено	6.	Выстроены	9.	Включающий
4.	Размещено	8.	Прикрепленный	12.	Связанный

4. Limitations

Limitations associated with the use of the technical terms database include the manual development and management of technical terminology and synonyms for it. At present, the technical terms database contains only selected terminology related to nanotechnology, and other variations of technical terms that may be present in patent literature have not been included yet. Translation issues across multiple languages may additionally reduce effectiveness due to different semantic meanings of technical terms across various languages. Moreover, the technical terms database functions mainly as a database of keywords.

5. Conclusion

In order to demonstrate the importance of terminology structure for automated patentability search engines, the following suggested technical term database was designed. The multilingual technical keywords contribute to the consistency between search queries and found patents in various patent databases.

Within the structure of the database, it is possible to perform: grouping of noun-based technical terminology; multilingual terminology mapping from Azerbaijani, English, and Russian; inclusion of a synonym-based query expansion mechanism; development of a search query generator.

The suggested technical term database is capable of improving the quality of prior art searches within specialized technical fields such as nanotechnologies.

The constructed multilingual technical database revealed that terminology standardization is critical to automatic patent retrieval systems. While creating the database, it was found that there are a lot of different technical terms in patents related to polymer nanotechnology in Azerbaijani, English, and Russian languages. Creating structured noun-based categories helped to solve the problem of translating technical expressions literally and having many terminological variants of one expression.

This study suggests that the construction of a technical database could also help to build further semantic retrieval systems by providing structured terminology databases that can be used in machine learning or expert systems. Although now, the database is focused on organizing keywords and synonyms, in the future, the database can become a part of more complex systems such as similar patents detection systems and others.

Author Contributions

The author was responsible for the conceptualization of the study, development of the research methodology, investigation, analysis and interpretation of the findings, preparation and revision of the manuscript, and approval of the final version for publication.

Conflict of Interest

The author declares no conflicts of interest.

Funding

This research received no external funding.

Acknowledgment

The author acknowledges Western Caspian University for providing institutional support and academic resources that contributed to the completion of this research.

Abbreviations

Natural Language Processing (NLP), International Patent Classification (IPC).

References

[1] Intellectual Property Agency of the Republic of Azerbaijan. Azerbaijan Patent Database [database]. Baku (Azerbaijan): Intellectual Property Agency of the Republic of Azerbaijan; [cited 2026 April 20]. Closed-access database.

[2] Federal Institute of Industrial Property (FIPS). Information Retrieval System (IPS) [Internet]. Moscow (Russia): Federal Institute of Industrial Property; [cited 2026 April 20]. Available from: https://www.fips.ru/iiss/db.xhtml

[3] Eurasian Patent Organization (EAPO). Eurasian Patent Information System (EAPATIS) [Internet]. Moscow (Russia): Eurasian Patent Organization; [cited 2026 April 20]. Available from: https://www.eapatis.com/

[4] World Intellectual Property Organization (WIPO). PATENTSCOPE [Internet]. Geneva (Switzerland): World Intellectual Property Organization; [cited 2026 April 20]. Available from: https://patentscope.wipo.int/search/en/search.jsf
[5] European Patent Office (EPO). Espacenet [Internet]. Munich (Germany): European Patent Office; [cited 2026 April 20]. Available from: https://worldwide.espacenet.com/patent/search
[6] United States Patent and Trademark Office (USPTO). Patent Public Search [Internet]. Alexandria (VA): United States Patent and Trademark Office; [cited 2026 April 20]. Available from: https://ppubs.uspto.gov/pubwebapp/
[7] Google Patents. Patent database [Internet]. [cited 2026 April 20]. Available from: https://patents.google.com/
[8] Patent haqqında: Azərbaycan Respublikasının Qanunu. Maddə 8 [Internet]. Bakı: Azərbaycan Respublikası; 1997 [cited 2026 April 20]. Available from: https://patent.copat.gov.az/files//262902927228350303613112-IQ%20Patent%20haqq%C4%B1nda%20(2).pdf
[9] Helmers L, Horn F, Biegler F, Oppermann T, Müller KR. Automating the search for a patent's prior art with a full text similarity search. PloS one. 2019 Mar 4;14(3):e0212103. https://doi.org/10.1371/journal.pone.0212103
[10] Risch J, Alder N, Hewel C, Krestel R. Patentmatch: a dataset for matching patent claims & prior art. arXiv preprint arXiv:2012.13919. 2020 Dec 27. https://doi.org/10.48550/arXiv.2012.13919
[11] Simian D, Şerban ME. Improving search query accuracy for specialized websites through intelligent text correction and reconstruction models. Information. 2024 Nov 1;15(11):683. https://doi.org/10.3390/info15110683
[12] Rzaguliyev A. Automation of patentability for inventions using multi-step automated search model. In: Proceedings of the International Conference on Recent Advances in Computer Science and Information Technology; 2026.
[13] PATENTSCOPE. Patent database [Internet]. Geneva: World Intellectual Property Organization (WIPO); [cited 2026 April 20]. Available from: https://patentscope.wipo.int/search/en/search.jsf
[14] Azərbaycan Respublikası Əqli Mülkiyyət Agentliyi, Patent və Əmtəə Nişanlarının Ekspertizası Mərkəzi. Patent, faydalı model və sənaye nümunələri [Internet]. 2026 [cited 2026 Apr 20]. Available from: https://patent.copat.gov.az/publish-Inventions-utility-models-and-industrial-examples

Journal of Nanotechnology and Innovative Materials

Research Article

Synthesis of a Novel Surface-Active Agent Based on Hexadecylamine and Ethylene Chlorohydrin for the Removal of Thin Oil Films from Water Surfaces

Tarana A. Poladova[1], **Aygun M. Isayeva**[1], **Tarana K. Guliyeva**[1], **Fidan M. Vakilova**[1], and **Mehriban E. Poladova**[2]

[1]Institute of Petrochemical Processes named after Academician Yusif Mammadaliyev, 30 Khojaly Avenue, Khatai District, AZ1025 Baku, Azerbaijan
[2]Institute of Geography of the Ministry of Science and Education of the Republic of Azerbaijan, 117 H. Javid Avenue, AZ1073 Baku, Azerbaijan

Received: 21.04.2026 Accepted: 22.05.2026 Published: 29.05.2026

https://doi.org/10.54414/OJDK2231

Abstract

A novel surface-active salt based on hexadecylamine and ethylene chlorohydrin was successfully synthesized. The composition and molecular structure of the synthesized salt were characterized by Fourier-transform infrared (FTIR) and UV–Visible (UV–Vis) spectroscopy, while its principal physicochemical properties were determined. Tensiometric measurements demonstrated the high surface activity of the synthesized salt at the air–water interface. The specific electrical conductivity of its aqueous solutions was measured using an electroconductometric method, confirming that the synthesized salt exhibits electrolyte behavior. The aggregate sizes of hexadecylethanolammonium chloride (HDEAC) in aqueous solutions at different concentrations were determined by dynamic light scattering (DLS), and the corresponding particle size distribution histograms were obtained.

Keywords: catanionic salts, FTIR, UV–Vis spectroscopy, hexadecylethanolammonium chloride, oil spill remediation, oil collection

1. Introduction

The removal of petroleum-derived contaminants from water surfaces is of paramount importance for environmental protection. When crude oil and petroleum products enter aquatic environments, they spread spontaneously under the combined influence of surface tension, wind, and wave action, forming thin oil films on the water surface. This spontaneous spreading process is accompanied by a reduction in the system's free energy proportional to the increase in the contaminated surface area and is characteristic of dispersed water–oil emulsion systems discharged into the hydrosphere through industrial wastewater. Regardless of the mechanism of film formation, such oil films pose a serious environmental threat because the surface microlayer of aquatic ecosystems serves as a critical habitat for the most sensitive organisms and for the early developmental and reproductive stages of numerous aquatic species. Furthermore, the presence of an oil film adversely affects gas exchange, heat transfer, and water exchange between the hydrosphere and the atmosphere, thereby disrupting the physicochemical and biological processes occurring at the air–water interface [1], [2].

As is well established, relatively thick oil films are typically removed from water surfaces by mechanical methods. However, in the case of thin oil films, physicochemical techniques have proven to be considerably more effective. The removal and recovery of thin oil films (up to 0.5 mm in thickness) from aquatic environments is of great environmental and economic importance, since the recovered oil can be recycled and reused [3], [4].

In this regard, oil-collecting and oil-dispersing reagents play a crucial role. Owing to spontaneous emulsification, dispersants disrupt the continuous oil film, thereby restoring water, gas, and heat exchange between the hydrosphere and the atmosphere while promoting the natural biochemical oxidation of finely dispersed oil droplets suspended within the water column. Consequently, oil dispersion has become a widely accepted approach as an effective approach for mitigating oil-film contamination on water surfaces. Dispersing formulations are particularly suitable for the remediation of large-scale oil spills.

Alternatively, oil films can be removed from water surfaces using oil-collecting agents. In many cases, the dispersing and oil-collecting effects of these reagents overlap, as certain formulations exhibit both properties simultaneously. The principal active components of both oil-collecting and dispersing formulations are surfactants (surface-active agents) [5], [6], [7], [8]. To be effective as oil-collecting reagents, surfactants should exhibit rapid spontaneous spreading over the water surface with a spreading pressure exceeding 30 mN m^{-1}, possess low volatility, demonstrate adequate solubility in both water and oil, and maintain high chemical stability under operating conditions.

Oil-dispersing and oil-collecting reagents offer several advantages over conventional methods used to combat oil pollution. These include high efficiency, the ability to be applied regardless of the location, timing, or environmental conditions of an oil spill, and ease of application. Such reagents are particularly effective in the removal of ultrathin oil films, for which conventional mechanical and many physicochemical remediation techniques are often ineffective.

For Azerbaijan, with its numerous water bodies that have been extensively contaminated by crude oil and petroleum products, the development and investigation of novel, highly efficient oil-dispersing and oil-collecting reagents remain a matter of considerable environmental importance. Such reagents are typically based on amphiphilic chemical compounds containing both hydrophobic and hydrophilic structural fragments. This dual functionality provides a strong affinity for both the oil phase and the aqueous medium, thereby ensuring their high efficiency in the remediation of oil-contaminated water surfaces [9], [10], [11], [12], [13], [14].

2. Materials and Methods

The present study describes the synthesis and characterization of a novel catanionic surfactant with oil-collecting properties.

For this purpose, hexadecylethanolammonium chloride (HDEAC) was synthesized according to the procedure described previously [7]. The surfactant was prepared by reacting hexadecylamine with ethylene chlorohydrin in an equimolar ratio. The reaction was carried out at 21 °C for 4–5 h. The reaction scheme is presented below:

$$C_{16}H_{33}NH_2 + HO(CH_2CH_2)Cl \longrightarrow C_{16}H_{33}-\overset{\overset{\displaystyle CH_2CH_2OH}{|}}{\overset{+}{N}}H_2 \; Cl^-$$

The synthesized hexadecylethanolammonium chloride (HDEAC) was obtained as a yellowish, viscous resin. The product was completely soluble in ethanol, whereas in water it formed a stable dispersion accompanied by the generation of abundant foam. The melting point of the synthesized salt was found to be above 200 °C.

The chemical composition and molecular structure of HDEAC were characterized by Fourier-transform infrared (FTIR) and UV–Visible (UV–Vis) spectroscopy. FTIR spectra (Figure 1) were recorded using an ALPHA FTIR spectrometer (Bruker, Germany) over the wavenumber range of 600–4000 cm^{-1}.

The surface tension (σ) of the synthesized catanionic surfactant, HDEAC, was measured at the air–water interface using a Du Noüy ring tensiometer (KSV Sigma 702, Finland). Aqueous surfactant solutions with concentrations ranging from 0.00025 to 0.1 wt.% were prepared using deionized water. After equilibration for 24 h, their surface tension was measured at 19 °C.

The specific electrical conductivity (κ) of the aqueous HDEAC solutions was determined using an Anion-402 conductivity meter (Russia). The conductivity of aqueous solutions with concentrations ranging from 0.001 to 0.1 wt.% was measured 48 h after their preparation.

3. Results and Discussion

The chemical composition and molecular structure of hexadecylethanolammonium chloride (HDEAC) were characterized by Fourier-transform infrared (FTIR) and UV–Visible (UV–Vis) spectroscopy. The corresponding FTIR and UV–Vis spectra are presented in Figures 1 and 2, respectively.

The FTIR spectrum of the synthesized HDEAC is shown in Figure 1. A broad absorption band at 3263.4 cm⁻¹ is attributed to the stretching vibrations of the hydroxyl (O–H) group. The absorption bands observed at 2921.7 and 2852.1 cm⁻¹ correspond to the asymmetric and symmetric C–H stretching vibrations of the CH_3 and CH_2 groups, respectively. The absorption band at 1663.0 cm⁻¹ is assigned to the stretching vibration of the carboxylate (C(O)O) group. The peak at 1577.8 cm⁻¹ is attributed to the $–NH_2^+CH_2–$ group. The bands at 1254.2 and 1148.1 cm⁻¹ are associated with the deformation vibrations of the C–H bonds in the methylene and methyl groups. The absorption peak at 834.1 cm⁻¹ corresponds to the C–OH stretching vibration, whereas the band at 701.8 cm⁻¹ is assigned to the deformation vibrations of the $(CH_2)_n$ alkyl chain.

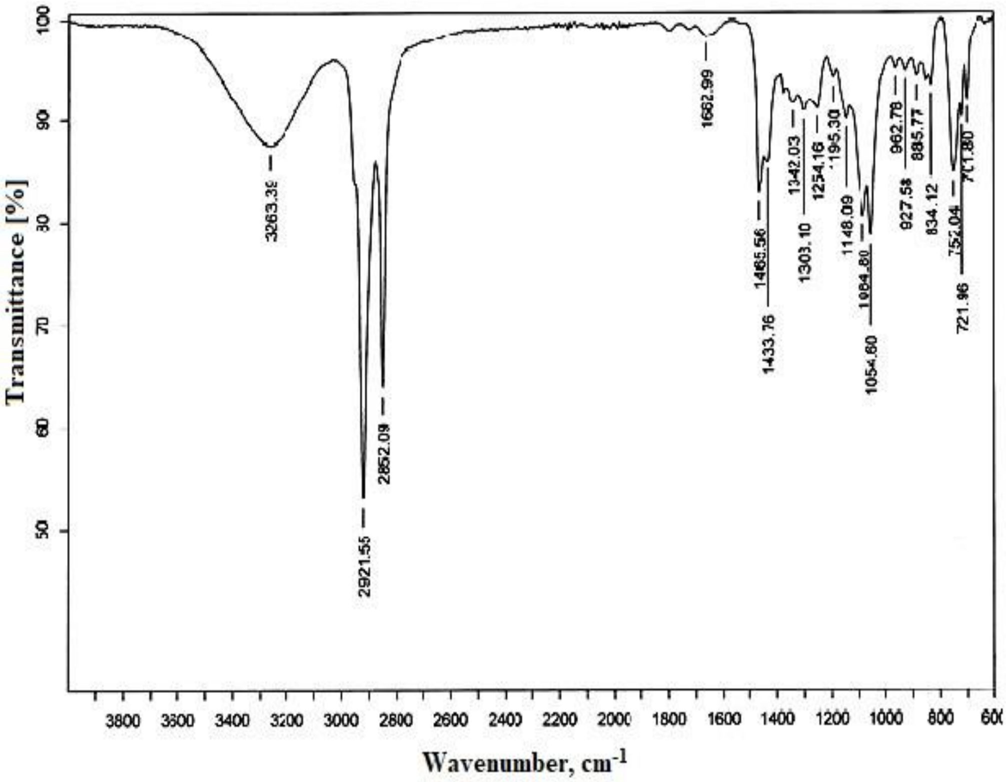

Figure 1. The FTIR spectrum of the HDEAC.

The absorption band at 211 nm is attributed to electronic transitions associated with the molecular structure of HDEAC (Figure 2).

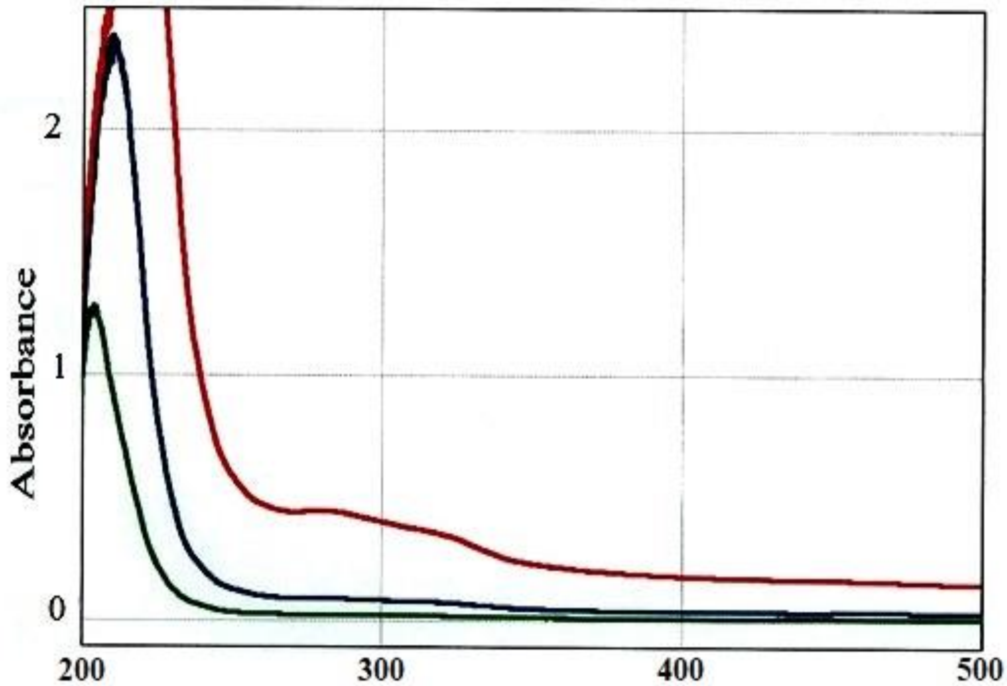

Figure 2. UV–Visible spectrum of HDEAC.

The electroconductometric analysis revealed that the specific electrical conductivity (κ) of aqueous HDEAC solutions increased monotonically with increasing surfactant concentration. As the concentration was raised from 0.02 to 0.7 wt.% at 19 °C, the conductivity increased from 60.2 to 226.0 µS cm^{-1}, whereas the conductivity of deionized water under the same conditions was 5 µS cm^{-1}. These findings confirm that the synthesized hexadecylethanolammonium chloride exhibits the characteristic behavior of an electrolyte in aqueous solution.

The results of the surface tension measurements demonstrated that the surface tension of pure water at the air–water interface was 72.1 mN m^{-1} at 19 °C. The synthesized HDEAC exhibited pronounced surface activity, confirming its excellent surface-active properties. In the presence of HDEAC, the surface tension decreased substantially from 72.1 mN m^{-1} (pure water) to 29.5 mN m^{-1}, indicating its strong ability to adsorb at the air–water interface and significantly reduce the interfacial free energy.

The oil-collecting performance of the synthesized compounds was evaluated under laboratory conditions according to the procedure described in Ref. [4]. Briefly, 40 mL of water and 1 mL of crude oil were introduced into a Petri dish. After the formation of a uniform oil film on the water surface, 0.02 g of the reagent (applied as an aqueous solution) was added, and the area of the oil slick collected into a compact spot (S_0) was measured immediately.

The experiments were carried out using distilled water, freshwater, and seawater (Caspian Sea water). Crude oil obtained from the Pirallahi oil field possessed a density of ρ_{20} = 0.924 g cm^{-3}. In the laboratory tests, crude oil from the Pirallahi oil field was spread over the surfaces of the three types of water: distilled water, freshwater, and seawater (Caspian Sea water), forming a thin oil film with a thickness of approximately 0.17 mm. The efficiency of the synthesized reagents was assessed by monitoring the reduction in the surface area of the oil slick following treatment with 5 wt.% aqueous solutions of the synthesized salts. Their oil-collecting performance was evaluated using two parameters: the oil-collection coefficient (K), defined as the ratio of the initial oil-film area to the area of the oil spot after treatment, and the oil retention time (τ), representing the duration for which the collected oil remained compact. The experimental results are summarized in Table 1.

Table 1. Oil-Collecting and Oil-Dispersing Performance of Hexadecylethanolammonium Chloride (HDEAC).

Reagent status	Distilled water		Fresh water		Sea water	
	τ, time	K	τ, time	K	τ, time	K
HDEAC						
100% product	0–0.5 1.0–2.0 3.0–15.0 24.0–168.0	30.9 55.2 60.8 80.6	0–0.5 1.0–2.0 3.0–15.0 24.0–168.0	35.1 43.2 55.7 60.8	0–0.5 1.0–2.0 3.0–15.0 24.0–168.0	38.4 55.3 60.8 80.6
5% product	0–0.5 1.0–2.0 3.0–168.0	35.4 42.5 79.2	0–0.5 1.0–2.0 3.0–168.0	46.1 55.9 60.7	0–0.5 1.0–2.0 3.0–168.0	43.6 65.5 80.6

As shown in Table 1, the synthesized surfactant exhibited excellent oil-collecting performance. Both the undiluted product and its 5 wt.% aqueous dispersion demonstrated high oil-collecting and oil-dispersing efficiencies. The maximum oil-collection coefficient (K) reached 80.6, while the reagent maintained its effectiveness for more than 168 h, indicating excellent long-term stability and sustained performance during oil spill remediation.

4. Conclusion

Hexadecylethanolammonium chloride (HDEAC) was successfully synthesized by the reaction of hexadecylamine with ethylene chlorohydrin. FTIR and UV–Vis analyses confirmed the formation of the target compound, while conductivity and surface tension measurements demonstrated its electrolyte behavior and high surface activity. Laboratory tests showed excellent oil-collection performance in distilled, fresh, and seawater, indicating that HDEAC is a promising surfactant for the remediation of thin oil films from contaminated water surfaces.

Author Contributions

All authors contributed to the conception, investigation, analysis, writing, and revision of the manuscript. All authors have read and approved the final version of the manuscript.

Conflict of Interest

The authors declare no conflicts of interest.

Funding

This research was not supported by external funding.

Acknowledgment

The authors express their gratitude to all individuals and institutions who supported this research and the preparation of the manuscript.

Abbreviations

Hexadecylethylammonium Chloride (HDEAC), Ultraviolet–Visible Spectrometer (UV–Vis spectrometer), Fourier-Transform Infrared (FTIR), Dynamic Light Scattering (DLS).

References

[1] Schramm LL. Fundamentals and applications in the petroleum Industry. Adv. Chem. 1992 May 5;231:3-24.

[2] Wang Z, Stout S. Oil spill environmental forensics: fingerprinting and source identification. Elsevier; 2010 Jul 26.

[3] Mariano AJ, Kourafalou VH, Srinivasan A, Kang H, Halliwell GR, Ryan EH, Roffer M. On the modeling of the 2010 Gulf of Mexico oil spill. Dynamics of Atmospheres and Oceans. 2011 Sep 1;52(1-2):322-40. https://doi.org/10.1016/j.dynatmoce.2011.06.001
[4] Гумбатов ГГ, Дашдиев РА. Применение ПАВ для ликвидации аварийных разливов нефти на водной поверхности. Баку: Элм. 1998;210:1.
[5] Humbatov, H. H.; Dashdiyev, R. A. Application of Surfactants for the Elimination (or Liquidation) of Oil Spills on the Water Surface. Baku: Elm Publishing House, 1998. 210 pp. (in Russian).
[6] Poladova TA. Synthesis and study of a new catanionic surface-active *n*-octylethanolammonium pentanoate salt. Processes of Petrochemistry and Oil Refining. 2022;23(1):155-161.
[7] Yu ZJ, Zhao GX. The physicochemical properties of aqueous mixtures of cationic-anionic surfactants: I. The effect of chain length symmetry. Journal of Colloid and Interface Science. 1989 Jul 1;130(2):414-20. https://doi.org/10.1016/0021-9797(89)90118-5
[8] Asadov ZH, Nasibova SM, Poladova TA, Rahimov RA, Asadova AZ. Petroleum collecting and petroleum dispersing reagents based on alkyl amine and alkyl iodides. Materials Research Innovations. 2012 Jun 1;16(3):175-8. https://doi.org/10.1179/1433075x11y.0000000055
[9] Sakai H, Okabe Y, Tsuchiya K, Sakai K, Abe M. Catanionic mixtures forming gemini-like amphiphiles. Journal of oleo science. 2011;60(11):549-55. https://doi.org/10.5650/jos.60.549
[10] Ahmadova GA, Abilova AZ, Rahimov RA, Askerzade SM, Asadov ZH, Zubkov FI, Ahmadbayova SF. Effect of alternation of chloropropoxy and propoxy units and impact of the ethylol-group number on properties of surfactants. Australian Journal of Chemistry. 2018 Nov 16;71(11):837-45. https://doi.org/10.1071/ch18213
[11] Yin H, Lin Y, Huang J. Microstructures and rheological dynamics of viscoelastic solutions in a catanionic surfactant system. Journal of Colloid and Interface Science. 2009 Oct 1;338(1):177-83. https://doi.org/10.1016/j.jcis.2009.05.076
[12] Asadov ZH, Poladova TA, Salamova NV. New surface-active polymer complexes based on dodecylammonium caprinate and pelargonate salts. Polish journal of science. 2020(23):15-21.
[13] Rahimov RA, Asadov ZH. Coconut oil fatty acid ammonium-type salts. Journal of Molecular Liquids. 2013 Jun 1;182:70-5. https://doi.org/10.1016/j.molliq.2013.03.013
[14] Rosen MJ. Surfactants and interfacial phenomena. 3rd ed. Hoboken (NJ): John Wiley & Sons; 2004.

Western Caspian University

Journal of Nanotechnology and Innovative Materials

Vol 1, No 4
May, 2026

Editorial Office Address: 17 A, Ahmad Rajabli Street,

III Parallel, Baku, Azerbaijan

Phone: +994 12 565 39 77

Email: jnim@wcu.edu.az

https://jnim.wcu.edu.az/

Submitted for collection: 06.04.2026

Signed for printing: 29.05.2026

Paper format: 60x84 1/16 17.75